IEEE Access
Multidisciplinary | Rapid Review | Open Access Journal

Received September 21, 2016, accepted October 17, 2016, date of publication November 1, 2016, date of current version March 8, 2017.

Digital Object Identifier 10.1109/ACCESS.2016.2623798

Non-Coherent Capacity of *M*-ary DCSK Modulation System Over Multipath Rayleigh Fading Channels

WEI HU[1], LIN WANG[1], (Senior Member, IEEE), GUOFA CAI[2], AND GUANRONG CHEN[3], (Fellow, IEEE)

[1]Department of Communication Engineering, Xiamen University, 361005 Fujian, China
[2]Department of Information Engineering, Guangdong University of Technology, 510006 Guangzhou, China
[3]Department of Electronic Engineering, City University of Hong Kong, Hong Kong

Corresponding author: L. Wang (wanglin@xmu.edu.cn)

This work was supported in part by the NSF of China under Grant 61271241 and in part by the Hong Kong Research Grants Council under GRF Grants CityU 11208515).

ABSTRACT Non-coherent capacity bounds for the M-ary differential chaos shift keying (DCSK) modulation system are derived and analyzed over multipath Rayleigh fading channels, deriving conditions on the channel state information/non-channel state information (CSI/NonCSI) and soft-decision/hard-decision (SD/HD), respectively. Meanwhile, the inter-symbol interference is modeled and analyzed mathematically. Through numerical simulations and analyses, it is found that: 1) the influences of the spreading factor β, multipath number L, modulation dimension M, CSI/NonCSI, and SD/HD on the non-coherent capacity bounds are significant; 2) there is a relatively broad range of code rates corresponding to the optimal system power in U-shaped capacity curves of the non-coherent reception; and 3) the U-shaped non-coherent capacity bounds are proven to exist by investigating the mechanism of the low density parity check coded the M-ary DCSK system. These results are useful as benchmarks for designing power-efficient coded M-ary DCSK systems.

INDEX TERMS Non-coherent capacity, soft/hard-decision (SD/HD), channel state information/non-channel state information (CSI/NonCSI), inter-symbol interference (ISI).

I. INTRODUCTION

Differential chaos shift keying (DCSK) modulation based ultra-wideband (UWB) technology is in research frontier of wireless personal area networks (WPANs) [1]–[4] because of its unique characteristics of wide-spectral carrier chaotic signals, low power, low correlation and anti-interference ability. This modulation technique offers an outstanding bit error rate (BER) performance on the multipath fading setting [5]–[7], which is attributed to its differential structure and results from overcoming the difficult synchronization problem without requiring channel state information (CSI) by the receiver [8].

Noticeably, it is a drawback that the DCSK system needs the radio frequency (RF) delay lines in the transceiver. Code-shifted DCSK (CS-DCSK) was proposed in [9] to improve the energy efficiency by spreading two chaotic slots with Walsh codes. Multi-carrier DCSK (MC-DCSK) system proposed in [10] can solve the delay line requirement problem and also enhance the spectrum efficiency and energy efficiency. In [11], a phase-separated DCSK (PS-DCSK) scheme was proposed by using the orthogonality of sine signal and cosine signal. Another drawback is that half bit duration is set as reference, resulting in the decreasing of data rate and energy efficiency. A differential DCSK (DDCSK) scheme in [12] and a reference-modulated DCSK (RM-DCSK) scheme in [13] were proposed to achieve a high data rate. The orthogonal multi-level DCSK (OML-DCSK) system was proposed in [14] to achieve a higher data rate and better BER performance. To achieve low power, a double-level multi-resolution DCSK system was proposed in [15] based on MC-DCSK and quadrature chaos shift keying (QCSK) [16]. In [17], M-ary DCSK, using chaotic basis functions and dividing the symbol period into four time slots, was designed to improve the data rate. Another scheme of M-ary DCSK system in [18] was presented to replace chaotic codes with Walsh codes. The BER derivation of the frequency

modulated (FM) version of the corresponding communication systems was studied in [18] and [19] over additive white Gaussian noise (AWGN) channels and it revealed that the *M*-ary DCSK modulation scheme suits to power-limited communication systems.

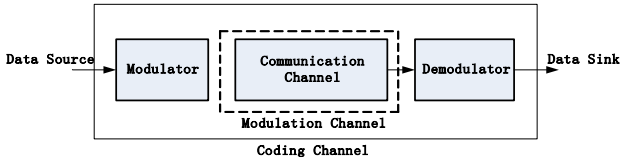

FIGURE 1. Block diagrams of coding channel and modulation channel.

It is now well known that the reliability of communication channels can be enhanced by some forward error correcting (FEC) codes for low power design [20]. The coding channel is described in Fig. 1, constituting of the modulator, the communication channel and the demodulator, which also shows the influence of the modulator-demodulator on the capacity bound. The product accumulate (PA) codes were combined with the single input multiple output (SIMO) FM-DCSK systems to obtain an outstanding BER performance in [21]. In [22] and [23], the low density parity check (LDPC) codes were incorporated to improve the overall performance of the DCSK system. Although these schemes are proposed to enhance the performances, they cannot be used to analyze and calculate the theoretical capacity limits directly for coding design.

Several works have been devoted to the study of the capacity, including systems with multipath channels. In [23], the achievable rate (output extrinsic mutual information) is simulated by numeric statistics on the log likelihood ratios (LLRs) for the *M*-ary DCSK communication system. Although it is not accurate, the nonlinear capacity exists, which is different from the conventional modulation systems. In [24], the capacity is analyzed and calculated in term of non-CSI demodulation over single-path Rayleigh fading channel for binary DCSK system, but ignoring the influence of inter-symbol interference, the soft/hard-decision, the channel state information, the dimension M and the fading path number L. The capacity and mutual information of a broadband fading channel consisting of a finite number of time-varying paths were investigated in [25]. In [26], the capacities of Gaussian and Webb channels were computed for modeling an optical channel using an avalanche photodiode detector (APD) and pulse-position modulation (PPM). In [27], the capacity of coherent reception of the *M*-ary DCSK system over AWGN channels was derived, which is independent of the spreading factor and different from the model of non-coherent reception to be studied in this paper.

But the above designs ignore the influences of multipath effect on the capacity bound. In [28], the capacity of a discrete-time Gaussian channel with inter-symbol interference (ISI) was derived, where the channel was mapped to an N-circular Gaussian channel. The ISI channel and the capacity limit were normalized in [29]. In [30] and [31], approximations of the capacity limit for ISI channels were proposed, introducing a Markovian achievable scheme. And a simulation-based technique was proposed in [32] and [33] to compute the information rates of soft-input soft-output (SISO) ISI channels with inputs selected from a finite alphabet.

In this paper, the non-coherent theoretical capacity bounds for the *M*-ary DCSK system are calculated and analyzed over multipath Rayleigh fading channels, taking into account the influences of soft/hard-decision and channel/non-channel state information. The aim is to achieve an energy-efficient design for coded chaotic modulation systems.

The main contributions of this paper are summarized as follows:

1) The general non-coherent capacity expressions of the *M*-ary DCSK modulations without inter-symbol interference over multipath Rayleigh fading channels are derived and analyzed accurately, and conditions on the SD/HD and CSI/NonCSI are established, respectively.

2) The capacity expressions of the *M*-ary DCSK modulations with inter-symbol interference are derived under various scenarios by considering the parameters of modulation dimension M, path number L, SD/HD and CSI/NonCSI, where the interference is modeled mathematically. These results can guide the designers to improve the performance of *M*-ary DCSK communication systems.

3) It is proven that U-shaped capacity bounds exist in the LDPC coding mechanism of the *M*-ary DCSK system at different code rates: $R_c = \frac{1}{3}, \frac{1}{2}, \frac{2}{3}$. Meanwhile, the capacity bounds of infinite fading path ($L \to \infty$, AWGN channels) and single-path ($L = 1$) are simulated and analyzed.

The organization of this paper is as follows. The influences of SD/HD, including CSI/NonCSI and ISI/NonISI interference, on capacity bounds are analyzed in Section II. In Section III, the non-coherent capacity bounds in various cases are derived and analyzed, along with some numerical simulations and discusses, in Section IV, where the U-shaped capacity bounds are proved to exist. Finally, Section V provides some concluding remarks.

II. SYSTEM MODEL AND NOTATIONS

The *M*-ary DCSK system model is shown in Fig. 2, which includes the modulator and non-coherent demodulator [23].

A. M-ary DCSK SYSTEM

Transmitter: the transmitter of the *M*-ary DCSK system is shown in Fig. 2(a). The delayed copies of the chaotic signal are multiplied by the elements of a Walsh function. These products are used to construct the transmitted signal. The Walsh functions are defined by the following recursive relation: $W_{2^n} = \begin{bmatrix} W_{2^{n-1}} & W_{2^{n-1}} \\ W_{2^{n-1}} & -W_{2^{n-1}} \end{bmatrix}$ and $W_{2^0} = [1]$, for $M = 2^n$, $n \geq 1$, and the transmitted signal is defined as a constant energy. Assuming that symbol m is transmitted, the transmitted signal

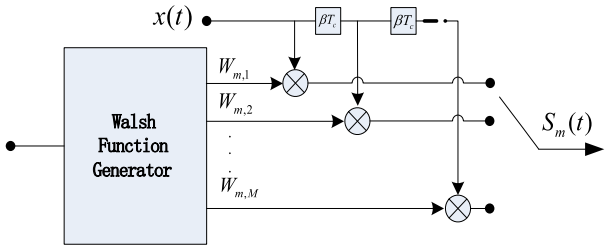

(a) M-ary DCSK system modulator.

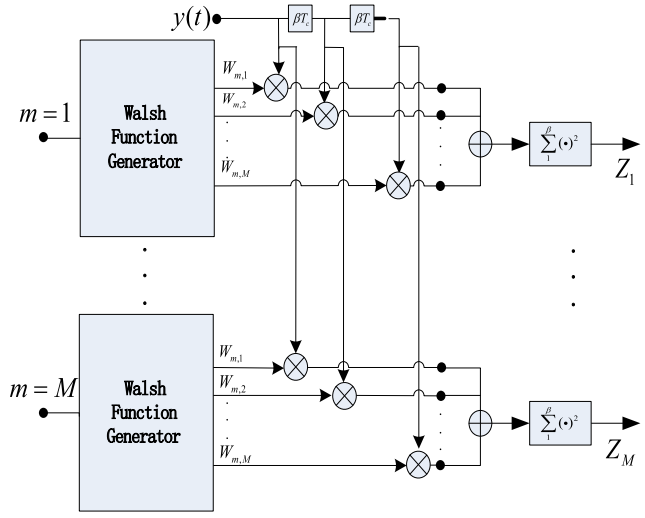

(b) Non-coherent demodulator.

FIGURE 2. Model of the M-ary DCSK modulation system. (a) M-ary DCSK system modulator. (b) Non-coherent demodulator.

for the M-ary DCSK modulation system is defined as follows:

$$S_m(t) = \sum_{k=1}^{M} \sum_{j=1}^{\beta} w_{m,k} x_{m,j} rect(t - k\beta T_c - jT_c). \quad (1)$$

where $rect(\cdot)$ is named by the rectangular wave function; $w_m = [w_{m,1}; w_{m,2}; ...; w_{m,M}]$ and $w_l = [w_{l,1}; w_{l,2}; ...; w_{l,M}]$ denote two arbitrarily chosen Walsh functions, which satisfy $\frac{1}{M}\sum_{k=1}^{M} w_{m,k} w_{l,k} = 1$ when $m = l$ or 0 when $m \neq l$; β is defined as the spreading factor; $x(t)$ denotes the chaotic signal, which satisfies $\int_0^{T_c} x(t)^2 dt = \frac{1}{M}$; T_c and βT_c present the chip duration and the bit duration of a basic chaotic signal, respectively.

Non-Coherent Reception: the non-coherent demodulator of the M-ary DCSK system is shown in Fig. 2(b), which has M Walsh functions and $M-1$ delay elements. In this demodulator, the received signal is likewise required to multiply with all the M Walsh functions. Differing from the coherent reception, the received signal is first fed into a delay line with delay T_c for non-coherent system. Then, the output signal of every delay element is multiplied with the corresponding element in each Walsh function. The products corresponding to one Walsh function are then summarized. The sum values are used to compute the energies $y_1, ..., y_M$, the received signal $y_m(t)$ is given by

$$y_m(t) = \sum_{l=1}^{L} \alpha_{l,m} S_m(t - \tau_l) + n(t) \quad (2)$$

where L is the path number, $\alpha_{l,m}$ and τ_l are the channel coefficient and the time delay of l-th path respectively.

Thus, for the non-coherent M-ary DCSK system, the observation value of the $\widehat{m}$-th auto-correlator is obtained as

$$z_{\hat{m}} = \sum_{j=1}^{\beta} \left[\sum_{k=1}^{M} \left(\sum_{l=1}^{L} \alpha_{l,m} w_{l,m,k} x_{m,(j-\tau_l)} \right) w_{\hat{m},k} + \sum_{k=1}^{M} w_{\hat{m},k} n_{k,j} \right]^2, \quad (3)$$

where $\alpha_{l,m}$ presents the l-th path channel coefficient when transmitting the m-th symbol; and $n_{k,j}$ are Gaussian noise variables with zero mean and variance σ^2.

B. CAPACITY ANALYSIS

In Fig. 1, the input X is modulated through a modulator and is then transmitted over the modulation channel. At the output side of the channel, the received signals are processed by the demodulator, thus a scalar or vector Y is obtained. The observation of the channel output Y provides an average bits of information about the input X, $I(X; Y)$, which is the mutual information between Y and X. For M-ary DCSK system, the Y is the observation of the auto-correlator for non-coherent demodulation. The capacity of the modulator over the modulation channel is the maximum amount of information that can be transmitted reliably, given by

$$C = \max_{p(X)} I(X; Y), \quad (4)$$

where the maximum mutual information is taken over the input probability distribution $p(X)$, providing the capacity for the communication system.

For soft-decision, the capacity of the channel with input signals $X = \{x_1, x_2, ..., x_M\}$ restricted to an M-ary signal constellation without restriction on the demodulator, i.e., the analog output $Y = \{-\infty, +\infty\}$, is given by

$$C = \max_{p(X)} I(X; Y) = \max_{p(x_i)} \sum_{i=1}^{M} \int_{-\infty}^{+\infty} p(y|x_i)\, p(x_i) \log_2 \frac{p(y|x_i)}{p(y)} dy, \quad (5)$$

where $x = (x_1; x_2; ...; x_M)$ is the transmitted signal vector, $y = (y_1; y_2; ...; y_M)$ is the received signal vector, $p(y_j|x_i)$ is the probability density function (PDF) of y conditioned on x_j, and $p(y) = \sum_{j=1}^{M} p(x_j) p(y|x_j)$ is the marginal PDF.

Thanks to the symmetry of the considered channel, the capacity is achieved with an equi-probable M-ary data distribution, $p(x = x_i) = \frac{1}{M}$, thus the soft-decision (SD) capacity

can be expressed as

$$C_{SD} = \log_2 M - E_{y|x_1}\left\{\log_2\left[\frac{\sum_{i=1}^{M} p\left(y|x_i\right)}{p\left(y|x_1\right)}\right]\right\}, \quad (6)$$

where $E_{y|x_1}\{\cdot\}$ is the expectation operator with respect to y conditioned on x_1, and C_{SD} denotes the SD capacity.

For hard-decision, the capacity with M-ary input, M-ary output and symmetric channel, is written as

$$C_{HD} = \log_2 M + \mathbf{p}_M \log_2\left[\frac{\mathbf{p}_M}{M-1}\right] + (1-\mathbf{p}_M)\log_2\left[1-\mathbf{p}_M\right], \quad (7)$$

where $\mathbf{p}_M$ is the probability of incorrect symbol detection, and C_{HD} denotes the HD capacity. As soon as the value $\mathbf{p}_M$ is obtained, the HD capacity can be determined. Assuming that the signal x_1 is transmitted, the probability of incorrect symbol detection can be obtained, as $\mathbf{p}_M = 1 - \mathbf{pr}\{y_j < y_1, \forall j \neq 1|x_1\}$, where $\mathbf{pr}\{\cdot\}$ is the probability operator. Since the events are not independent due to the existence of the random variable y_1 in all of them, one can add a condition on y_1 to make these events independent:

$$\mathbf{p}_M = 1 - \int_{-\infty}^{\infty}\{\mathbf{pr}[y_j < y_1|y_1]\}^{M-1} p(y_1|x_1)dy_1. \quad (8)$$

Therefore, to obtain the HD capacities, the PDFs $p(y_i|x_i)$ of y_i and $p(y_i|x_j)$ of y_i, conditioned on x_j, must be calculated.

C. CHANNEL STATE INFORMATION

As is well known, channel state information can have a substantial influence on the fading channel capacity, which the CSI can use to optimize the transmitted power at the transmitter so as to increase the information rate. However, the difference between the capacity curves under transceiver CSI[1] and receiver CSI[2] are negligible in all cases [34]. So, in the following, it is assumed that the system is modeled based only on the receiver CSI.

D. INTER-SYMBOL INTERFERENCE ANALYSIS

As analyzed in Part A, for a multipath Rayleigh fading channels, the observation value of the $\hat{m}$-th auto-correlator is obtained as shown in (3). Generally, the ISI-noise has a significant impact on the performance, especially in the calculation of the capacity bounds. So, one cannot ignore the ISI, where the largest multipath time delay should not be set shorter than the chaotic signal duration, thus

$$z_{\hat{m}} = \begin{cases} \sum_{j=1}^{\beta}\left\{\sum_{l=1}^{L}\left(M_l\alpha_{l,m}x_{m,(j-\tau_l)}\right)^2\right\} + N + Q_m, & \hat{m} = m \\ \sum_{j=1}^{\beta}\left(\sum_{k=1}^{M} w_{\hat{m},k}n_{k,j}\right)^2, & \hat{m} \neq m, \end{cases} \quad (9)$$

where $M_l = \sum_{k=1}^{M} w_{l,m,k}w_{\hat{m},k}$, τ_l is the delay time of the l-th path and N is the channel noise, satisfying

$$\begin{cases} N = 2\sum_{j=1}^{\beta}\left[\left(\sum_{l=1}^{L} M_l\alpha_{l,m}x_{m,(j-\tau_l)}\right)\left(\sum_{k=1}^{M} w_{\hat{m},k}n_{k,j}\right)\right] + \sum_{j=1}^{\beta}\left(\sum_{k=1}^{M} w_{\hat{m},k}n_{k,j}\right)^2 \\ Q_m = \sum_{j=1}^{\beta}\sum_{l=1}^{L}\sum_{\substack{s=1 \\ s\neq l}}^{L}\left(\left[\alpha_{l,m}x_{m,(j-\tau_l)}\right]\left[\alpha_{s,m}x_{m,(j-\tau_s)}\right]\right) \\ Y_m = \sum_{j=1}^{\beta}\left\{\sum_{l=1}^{L}\left(M_l\alpha_{l,m}x_{m,(j-\tau_l)}\right)^2\right\} + N, \end{cases} \quad (10)$$

where Q_m is the ISI-noise, which results from the multipath-effect but is useless for available signals, and Y_m is defined by the output of the auto-correlator without ISI. For the receiver, the ISI-noise and N are both interference noises.

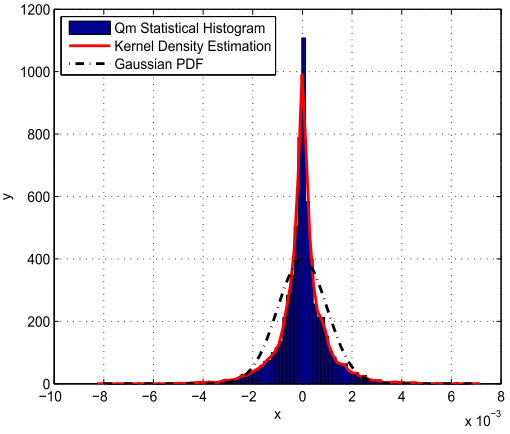

FIGURE 3. Data statistics of ISI-noise Q_m.

III. NON-COHERENT CAPACITY OF THE *M*-ARY DCSK SYSTEM

In this section, the non-coherent capacity bounds of the M-ary DCSK with/without ISI are calculated and analyzed under the conditions of CSI-SD, CSI-HD, NonCSI-SD and NonCSI-HD, respectively.

Because of the serious influence of the ISI on the performance of the M-ary DCSK system, although the PDF is difficult to calculate, one can analyze the ISI-noise individually to obtain data statistics of the ISI-noise Q_m, as shown in Fig. 3. It is found that the envelope curve of the statistics is similar to a Gaussian distribution:

$$f_0\left(y_m\right) = \frac{1}{\sqrt{2\pi}\sigma_0}\exp\left(-\frac{y_m^2}{2\sigma_0^2}\right), \quad (11)$$

[1] transceiver CSI, both for transmitter and receiver.
[2] receiver CSI, only for receiver.

where σ_0 is the variance of ISI-noise. Then, it can be verified that the transition probability $p_{ISI}\left(\mathbf{z}|x_{\hat{m}}, \alpha_{l,m}\right)$ of the receive signal is the convolution value of the traditional channel transition probability and the ISI-probability, given by

$$p_{ISI}(\mathbf{z}|x_{\hat{m}}, \alpha_{l,m}) = p_{NonISI}(\mathbf{z}|x_{\hat{m}}, \alpha_{l,m}) * f_0(y_m), \quad (12)$$

where $p_{NonISI}(\mathbf{z}|x_{\hat{m}}, \alpha_{l,m})$ is generated for the traditional Non-ISI system, when $\sum_{j=1}^{\beta} x_{m,(j-\tau_l)} \cdot x_{m,(j-\tau_s)} \neq 0, l \neq s$ at $0 < \tau_L \ll \beta T_c$. So, the PDF of the multipath NonISI fading channels of the M-ary DCSK system is

$$\overline{p}(\mathbf{z}|x_{\hat{m}}, \alpha_{l,m}) = p_{NonISI}(\mathbf{z}|x_{\hat{m}}, \alpha_{l,m}), \quad (13)$$

where $\overline{p}(\mathbf{z}|x_{\hat{m}}, \alpha_{l,m})$ is defined as the NonISI-existed, differing from the PDF of ISI-existed. Emphatically, the influence of β on the capacity bounds will be considered in the M-ary DCSK system over multipath Rayleigh fading channels on all conditions.

A. SOFT-DECISION DEMODULATION WITH CSI

Mainly benefited from anti-multipath fading, the chaotic communication system is built with a spreading spectrum scheme. So, one should also analyze the effect of the spreading factor β on the non-coherent capacity bounds with ISI.

Assuming that $m = 1$. The decision vector can be expressed as $y = (y_1; y_2; ...; y_M)$, where y_1 is a statistically independent non-central chi-square random variable with β degrees of freedom and non-centrality parameter $s^2 = ME_s$, and $y_2, y_3, ..., y_M$ are all statistically independent central chi-square random variables with β degrees of freedom. Given a transmitted signal x_j, the decision variables are written respectively as follows: if the signal is present, $y_m \sim \chi^2(\beta, s^2)$; if the signal is absent, $y_{\hat{m}} \sim \chi^2(\beta)$, where $\chi^2(\cdot)$ denotes the chi-square distribution. Thus, the conditional PDFs of y_m are given by

$$p\left(y_m|x_{\hat{m}}, \alpha_{l,m}\right) = \left(\frac{1}{MN_0}\right)\left(\frac{y_m}{ME_s\theta_{l,m}}\right)^{\frac{\beta-2}{4}} \cdot \exp\left(-\frac{ME_s\theta_{l,m} + y_m}{MN_0}\right) \cdot I_{\left(\frac{\beta}{2}-1\right)}\left(\frac{2\sqrt{y_m ME_s\theta_{l,m}}}{MN_0}\right), \quad y_m \geq 0, \quad m = \hat{m}, \quad (14)$$

and

$$p\left(y_m|x_{\hat{m}}, \alpha_{l,m}\right) = \left[\frac{y_m^{\frac{\beta}{2}-1}}{(MN_0)^{\frac{\beta}{2}}\Gamma\left(\frac{\beta}{2}\right)}\right] \cdot \exp\left(-\frac{y_m}{MN_0}\right), \quad y_m \geq 0, \ m \neq \hat{m}, \quad (15)$$

where $I_n(\cdot)$ denotes the n-th Bessel function of the first kind, and the fading factor $\theta_{l,m} = \Sigma_{l=1}^{L}\alpha_{l,m}^2$. So, the conditional PDF for the received vector y can be written as

$$p(y|x_{\hat{m}}, \alpha_{l,m}) = p(y_{\hat{m}}|x_{\hat{m}}, \alpha_{l,m}) \prod_{\substack{m=1 \\ m\neq\hat{m}}}^{M} p(y_m|x_{\hat{m}}, \alpha_{l,m}). \quad (16)$$

Attentively, if the AWGN channels are selected for the non-coherent M-ary DCSK, equation (16) becomes

$$p(y|x_{\hat{m}}, \alpha_{l,m}) = \left(\frac{1}{MN_0}\right)\left(\frac{y_m}{ME_s}\right)^{\frac{\beta-2}{4}} \cdot \exp\left(-\frac{ME_s + y_m}{MN_0}\right) I_{\left(\frac{\beta}{2}-1\right)}\left(\frac{2\sqrt{y_m ME_s}}{MN_0}\right) \cdot \prod_{\substack{m=1 \\ m\neq\hat{m}}}^{M} \frac{y_m^{\frac{\beta}{2}-1}}{(MN_0)^{\frac{\beta}{2}}\Gamma\left(\frac{\beta}{2}\right)} \exp\left(-\frac{y_m}{MN_0}\right). \quad (17)$$

where the AWGN channels capacity can be judged by the multipath Rayleigh fading channels when L is infinite. Thus, the non-coherent capacity of M-ary DCSK system over AWGN channels can be considered as a particular case of the general multipath channels of DCSK system when the path number is increasing to infinity.

So, for the general multipath fading channels, we obtain

$$\begin{aligned} & p_{ISI}(\mathbf{z}|x_{\hat{m}}, \alpha_{l,m}) \\ &= p_{NonISI}(\mathbf{z}|x_{\hat{m}}, \alpha_{l,m}) * f_0(y_m) \\ &= p(\mathbf{y}|x_{\hat{m}}, \alpha_{l,m}) * f_0(y_m) \\ &= [p\left(y_{\hat{m}}|x_{\hat{m}}, \alpha_{l,m}\right) \prod_{\substack{m=1 \\ m\neq\hat{m}}}^{M} p\left(y_m|x_{\hat{m}}, \alpha_{l,m}\right)] * f_0(y_m) \\ &= \left[\left(\frac{1}{MN_0}\right)\left(\frac{y_m}{ME_s\theta_{l,m}}\right)^{\frac{\beta-2}{4}} \exp\left(-\frac{ME_s\theta_{l,m} + y_m}{MN_0}\right) \cdot I_{\left(\frac{\beta}{2}-1\right)}\left(\frac{2\sqrt{y_m ME_s\theta_{l,m}}}{MN_0}\right) \prod_{\substack{m=1 \\ m\neq\hat{m}}}^{M} \frac{y_m^{\frac{\beta}{2}-1}}{(MN_0)^{\frac{\beta}{2}}\Gamma\left(\frac{\beta}{2}\right)} \cdot \exp\left(-\frac{y_m}{MN_0}\right)\right] * f_0(y_m). \end{aligned} \quad (18)$$

Considering equation (6), based on the soft-decision demodulation and the receiver CSI, the receiver can get the CSI and the transceiver can also obtain the channel distribution information (CDI). In this case, one can derive the non-coherent capacity of ISI channel as follows:

$$\begin{aligned} & C_{CSI-SD} \\ &= \log_2 M - E_{\mathbf{z}|x_1}\left\{\log_2\left[\frac{\sum_{m=1}^{M} p\left(\mathbf{z}|x_m\right)}{p\left(\mathbf{z}|x_1\right)}\right]\right\} \\ &= \log_2 M \\ &\quad - E_{\mathbf{z}|x_1}\left\{\log_2\left[\frac{\int_{\alpha_{l,m}} \sum_{l=1}^{L} \sum_{m=1}^{M} p_{ISI}\left(\mathbf{z}|x_m, \alpha_{l,m}\right) f(\alpha_{l,m}) d\alpha_{l,m}}{\int_{\alpha_{l,m}} \sum_{l=1}^{L} p_{ISI}\left(\mathbf{z}|x_1, \alpha_{l,m}\right) f(\alpha_{l,m}) d\alpha_{l,m}}\right]\right\}. \end{aligned} \quad (19)$$

B. HARD-DECISION DEMODULATION WITH CSI

For the hard-decision case, the coding channel can be mapped to a symmetric channel of M-ary input and M-ary output for simplification, but its performance can be downgraded, as

$$C_{CSI-HD} = \log_2 M + \mathbf{p}_{CSI} \log_2 \left[\frac{\mathbf{p}_{CSI}}{M-1}\right] + (1-\mathbf{p}_{CSI}) \log_2 [1-\mathbf{p}_{CSI}], \quad (20)$$

where $\mathbf{p}_{CSI}$ is the probability of having an incorrect symbol, so the HD capacity should be based on the PDF of $\mathbf{p}_{CSI}$. When the hard-decision is employed, the detector can operate the DCSK symbol decision on the demodulator, but not on individual soft counts. Assuming that symbol x_1 is transmitted into the channel, the probability of incorrect symbol detection is given by $\mathbf{p}_{CSI} = 1 - \mathbf{pr}\{z_m < z_1; \forall m = 1|z_1\}$ in the $\{z_m\}$ used for determining the capacities of the multipath Rayleigh fading channels. So, the incorrect symbol PDF is given by

$$\begin{aligned}
&\mathbf{p}_{CSI} \\
&= 1 - \int_0^\infty \left\{ \sum_{l=1}^{L} \left[\int_0^{z_1} \int_0^\infty p_{NonISI}(z_m|x_{\hat{m}}, \alpha_{l,m}) d\alpha_{l,m} dz_m \right]^{M-1} \right. \\
&\qquad \left. \cdot\, p_{NonISI}(z_1|x_1, \alpha_{l,m}) \right\} * f_0(y_m) dz_1 \\
&= 1 - \int_0^\infty \left\{ \sum_{l=1}^{L} \left[\int_0^{y_1} \int_0^\infty p_{NonISI}(y_m|x_{\hat{m}}, \alpha_{l,m}) d\alpha_{l,m} dy_m \right]^{M-1} \right. \\
&\qquad \left. \cdot\, p_{NonISI}(y_1|x_1, \alpha_{l,m}) \right\} * f_0(y_m) dy_1, \quad (21)
\end{aligned}$$

where $\alpha_{l,m}$ denotes the fading factor of the l-th path.

C. SOFT-DECISION DEMODULATION WITHOUT CSI

For this case without CSI, the receiver cannot get the fading coefficient $\alpha_{l,m}$ when the symbols are output from the channel, so its PDF $p_{NonISI}(z_m|x_{\hat{m}})$ should be defined as

$$\begin{cases} p_{NonISI}(z_m|x_{\hat{m}}) = \int_0^\infty p(y_m|x_{\hat{m}}, \alpha_{l,m}) f(\alpha_{l,m}) \quad d\alpha_{l,m}, & \\ & m = \hat{m} \\ p_{NonISI}(z_m|x_{\hat{m}}) = p(y_m|x_{\hat{m}}, \alpha_{l,m}), & m \neq \hat{m}, \end{cases} \quad (22)$$

where the PDF does not include the fading coefficient $\alpha_{l,m}$ when $m \neq \hat{m}$, so the integral of the chi-square distribution based on $\alpha_{l,m}$ is itself.

In summary, the PDF of the entire sequence is

$$\begin{aligned}
&p(\mathbf{z}|x_{\hat{m}}) \\
&= p_{NonISI}(z_m|x_{\hat{m}}) * f_0(y_m) \\
&= [p(y_{\hat{m}}|x_{\hat{m}}) \prod_{\substack{m=1 \\ m\neq\hat{m}}}^{M} p(y_m|x_{\hat{m}})] * f_0(y_m) \\
&= \left[\left(\frac{1}{MN_0}\right) \left(\frac{y_m}{ME_s\theta_{l,m}}\right)^{\frac{\beta-2}{4}} \exp\left(-\frac{ME_s\theta_{l,m} + y_m}{MN_0}\right) \right. \\
&\qquad \left. \cdot I_{\left(\frac{\beta}{2}-1\right)} \left(\frac{2\sqrt{y_m ME_s\theta_{l,m}}}{MN_0}\right) \prod_{m=1, m\neq\hat{m}}^{M} p(y_m|x_{\hat{m}}) \right] * f_0(y_m), \quad (23)
\end{aligned}$$

where $I_n(\cdot)$ denotes the n-th Bessel function of the first kind. So, the capacity bound of SD demodulation without CSI is

$$\begin{aligned}
&C_{NonCSI-SD} \\
&= \log_2 M - E_{\mathbf{z}|x_1} \\
&\quad \times \left\{ \int_0^\infty p(z_1|x_m) \log_2 \left[\frac{1 + \sum_{m=2}^{M} p(\mathbf{z}|x_m)}{p(\mathbf{z}|x_1)} \right] dz_1 \right\}. \quad (24)
\end{aligned}$$

D. HARD-DECISION DEMODULATION WITHOUT CSI

As analyzed in Parts *B* and *C*, Section II, the probability of having an incorrect symbol in the NonCSI-receiver is given by

$$\begin{aligned}
\mathbf{p}_{NonCSI} &= 1 - \int_0^\infty \int_0^\infty \left\{ \sum_{l=1}^{L} \left[\int_0^{y_1} p(y_m|x_{\hat{m}}, \alpha_{l,m}) dy_m \right]^{M-1} \right. \\
&\qquad \left. .p(y_1|x_1, \alpha_{l,m}) * f_0(y_m) \right\} d\alpha_{l,m} dy_1, \quad (25)
\end{aligned}$$

So, the capacity of HD demodulation without CSI is given by

$$C_{NonCSI-HD} = \log_2 M + \mathbf{p}_{NonCSI} \log_2 \left[\frac{\mathbf{p}_{NonCSI}}{M-1}\right] + (1-\mathbf{p}_{NonCSI}) \log_2 [1-\mathbf{p}_{NonCSI}]. \quad (26)$$

IV. NUMERICAL RESULTS AND DISCUSSIONS

In this section, numerical results on the capacity bounds of the M-ary DCSK modulation over multipath Rayleigh fading channels are presented via Monte-Carlo simulation. It shows that U-shaped non-coherent capacity bounds exist by investigating the mechanism of the LDPC coded M-ary DCSK system.

A. NON-COHERENT CAPACITY OF THE M-ARY DCSK SYSTEM

The non-coherent capacity bounds of the M-ary DCSK system over a multipath Rayleigh fading channels in Fig. 4 and Fig. 5, where they show the ISI capacities and NonISI ones, respectively.

Fig. 4 shows the capacity bounds of the M-ary DCSK system without ISI. Figs. 4(a)-(d) show the capacities under the conditions of CSI-SD, CSI-HD, NonCSI-SD and NonCSI-HD. Firstly, the capacity bounds are left-shifted with the increasing of the modulation dimension M, and the overall

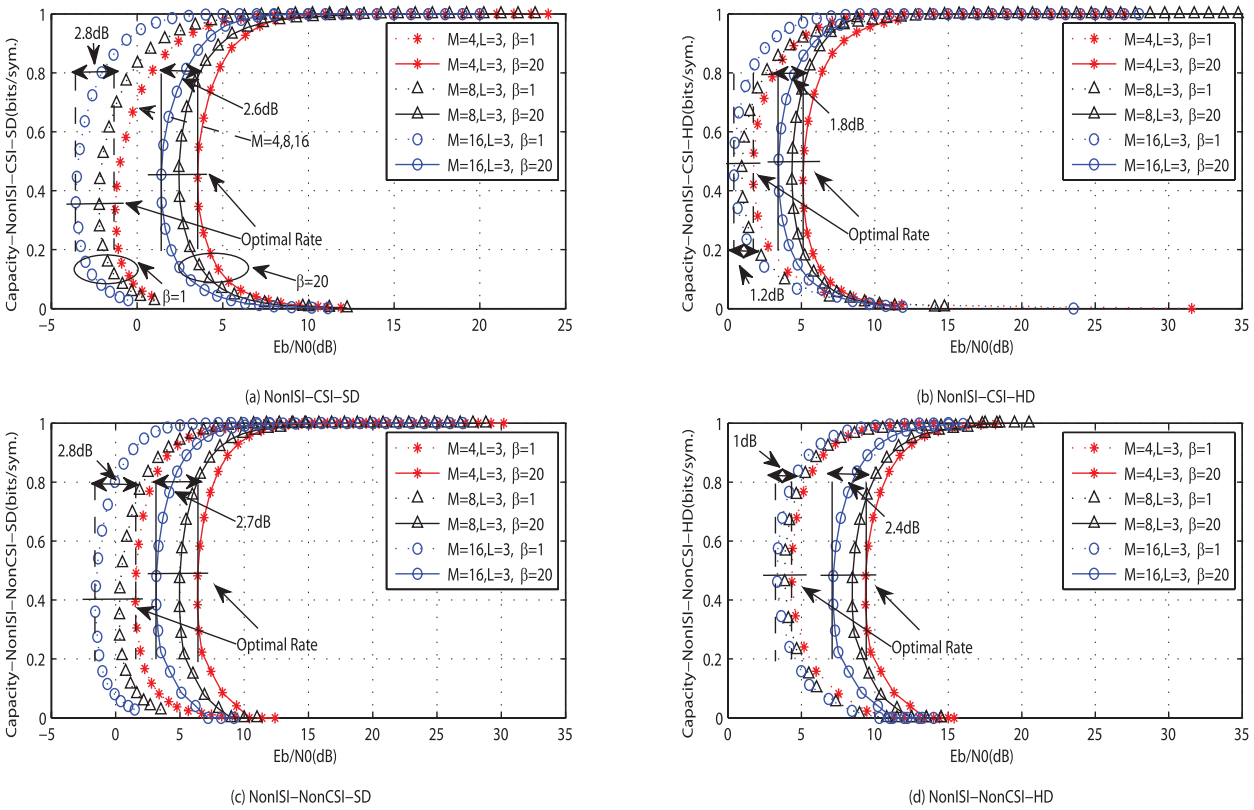

FIGURE 4. Non-coherent capacity bounds of the M-ary DCSK system over multipath fading channels without ISI.

power of the DCSK system becomes lower. By examining the vertical lines (including the solid lines and dashed lines), it can be concluded that the dimension's influence on the SD capacity is much stronger than in the HD case. For the CSI-existing capacity bounds shown in Fig. 4(a), the distance of lowest SNRs between $M = 4$ and $M = 16$ at spreading factor $\beta = 1$ is about 2.8dB, and 2.6dB for $\beta = 20$, where the distances are almost equal. But, in Fig. 4(b), the distances are about 1.2dB and 1.8dB, where the distance is larger when the spreading factor β is increasing. The same for the capacity bounds without NonCSI in Fig. 4(c) and Fig. 4(d): the distances are about 2.8dB and 2.7dB for NonISI-NonCSI-SD M-ary DCSK in Fig. 4(c), while they are about 1dB and 2.4dB for NonISI-NonCSI-HD M-ary DCSK in Fig. 4(d). On the contrary, the capacity curves move to the right (the capacity performance is worsened), when the spreading factor β is higher.

Besides, it is found that the influence of the spreading factor β on the HD capacity is much heavier than that is on the SD one. For example, in Fig. 4(a), the distances of lowest SNRs between $M = 4$ and $M = 16$, about 2.8dB and 2.6dB, are nearly identical, while the distance is larger from 1.2dB to 1.8dB in Fig. 4(b), with the increasing of the spreading factor β, so the difference between SD and HD is obvious.

More importantly, with the increasing of dimension M, it is clear that the capacity bound based on CSI-SD demodulation outperforms that of the schemes in NonCSI-SD and CSI-HD demodulations, where the NonCSI-HD system has the highest power consumption. When $M = 16, L = 3$, $\beta = 20$, the lowest bit-signal noise ratios (SNRs) corresponding to the optimal rate are about 1.5dB and 6.8dB for CSI-SD and NonCSI-HD, respectively, meanwhile the lowest for NonCSI-SD is about 3.2dB, and is about 3.5dB for the CSI-HD case.

Moreover, for the SD-exiting capacity bounds shown in Fig. 4(a) and Fig. 4(c), the optimal rate is larger when β is larger, but the optimal rate is still at about 0.5bits/sym for the HD-existing capacity shown in Fig. 4(b) and Fig. 4(d), owing to the symmetric channel of the M-ary input and M-ary output system. Lastly, it can be seen that the optimal rate is irrelevant to the enlargement of dimension M.

Fig. 5 presents the capacity bounds of the M-ary DCSK system with ISI. Because of the influence of ISI, the BER performance of ISI M-ary DCSK system can be worse, and the capacity performance is right-shifted comparing with the NonISI one. The same for Fig. 4: the U-shaped capacity curves are left-shifted (the power consumption is lower) with the increasing of the dimension M, but the dimension's influence on SD/HD capacity limits is much heavier than that is in the NonISI setting.

In Fig. 5(a), the distances of the lowest SNRs between $M = 4$ and $M = 16$ with different values of the spreading factor β,

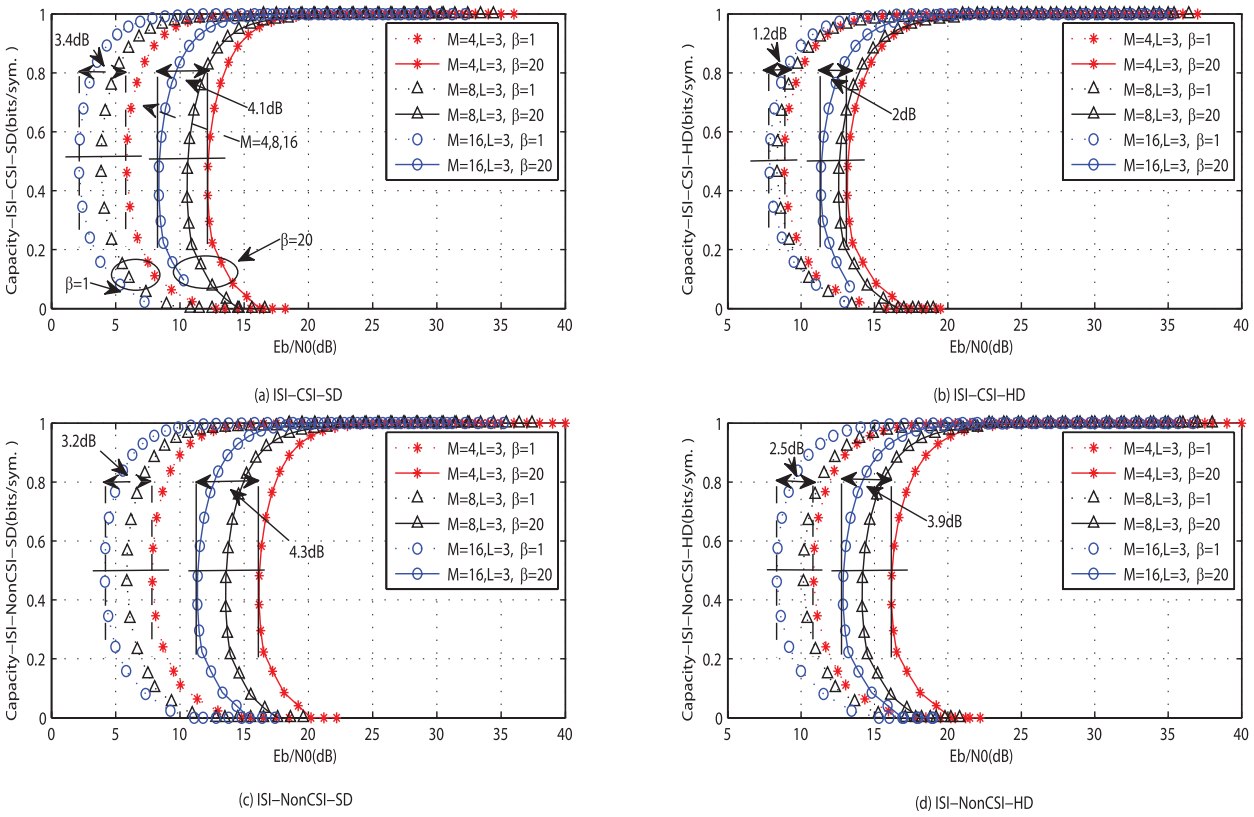

FIGURE 5. Non-coherent capacity bounds of the *M*-ary DCSK system over multipath fading channels with ISI.

about 3.4dB and 4.1dB, are larger than the cases when they are about 1.2dB and 2dB, as shown in Fig. 5(b). Meanwhile, the influence of the dimension M on the capacity bounds is heavier in this case. In Fig. 5(a), the distance is about 3.4dB between $M = 4$ and $M = 16$ at $\beta = 1$, while it is about 4.1dB at $\beta = 20$.

Also, the U-shaped bound is right-shifted (the power is increased) with a larger spreading factor β. Eventually, the optimal rate of the ISI capacity bounds is not affected by the dimension M and the spreading factor β. For pursuing the lowest power over multipath Rayleigh fading channels in practice, the NonISI-SD strategy for the capacity bounds should be chosen as a reference, where the optimal rate may stay at around $R_c = \frac{1}{2}$ for a broad range of code rates.

B. SIMULATION PROOFS AND DISCUSSIONS

To verify the existence of the U-shaped capacity bounds, the *M*-ary DCSK modulation system with low-density parity-check (LDPC) codes is simulated with three kinds of protograph LDPC as shown in TABLE 1.

Fig. 6(a) shows the BER performance of the verification mechanism of the LDPC coded *M*-ary DCSK system over multipath fading channels without ISI and CSI, and distances of performance at BER=10^{-6}. The average power gains of the three paths are $\rho_1 = \frac{4}{7}$, $\rho_2 = \frac{2}{7}$ and $\rho_3 = \frac{1}{7}$ with time delays $\tau_1 = 0$, $\tau_2 = 3$ and $\tau_3 = 5$, respectively. Meanwhile, the

TABLE 1. Three kinds of protograph LDPC codes.

R_c	Protograph LDPC	Code Length (bits)	Maximum Iteration Number
$\frac{1}{3}$	accumulate-repeat-by-jagged accumulate (ARJA) code	504	50
$\frac{1}{2}$	accumulate-repeat-by-4-jagged accumulate (AR4JA) code	500	50
$\frac{2}{3}$	accumulate-repeat-by-4-jagged accumulate (AR4JA) code	490	50

modulation scheme is selected with $M = 16$ and spreading factor $\beta = 80$ (which ignores the interference of ISI, $0 < \tau_L \ll \beta T_c$). It is found that the BER performance at $R_c = \frac{1}{2}$ outperforms the other two rates at BER=10^{-6}, where a gain of 0.6dB can be obtained comparing with $R_c = \frac{1}{3}$, and 0.55dB with $R_c = \frac{2}{3}$.

Fig. 6(b) presents a broad range of code rates and the relationship between capacity bound and BER performance. The solid straight lines with "△", "∗" and "○" denote the system powers based on the different rates at BER=10^{-6}, ($\frac{1}{3}$, 14.8dB), ($\frac{1}{2}$, 14.2dB), ($\frac{2}{3}$, 14.75dB).

And the cures with "⋆", "□", and "+" express the theoretical capacity bound, iterative receiver system (IR) capacity bound and non-iterative receiver system (NonIR) capacity bound, respectively. It can be seen that the difference of BER performance between the code rate at $R_c = \frac{1}{3}$ and $R_c = \frac{2}{3}$ is negligible in the 16-ary DCSK system, where

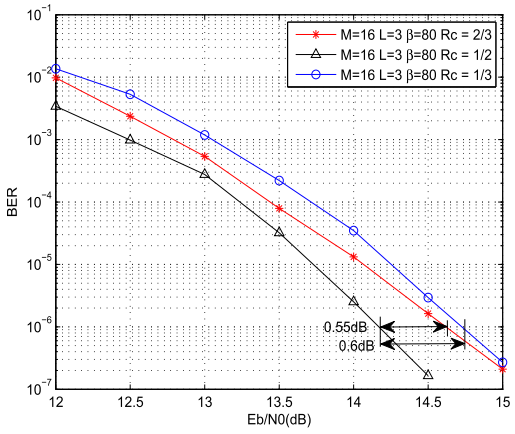

(a)

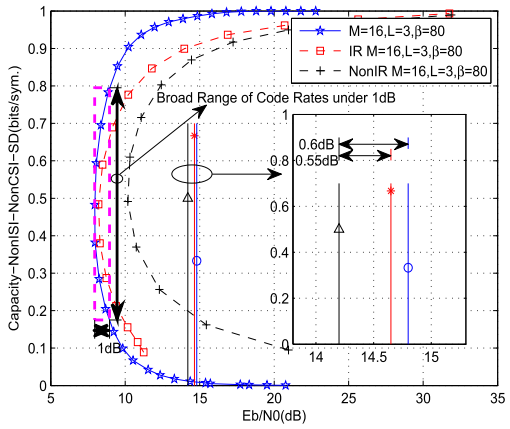

(b)

FIGURE 6. Existence verification of U-shaped capacity bounds of the M-ary DCSK system over multipath fading channels. (a) BER performance of the LDPC coding mechanism of the M-ary DCSK system with different code rates ($\frac{1}{3}$, $\frac{1}{2}$, $\frac{2}{3}$), and distances of performance at BER=10^{-6}. (b) Broad range of code rates and relationship between U-shaped bound and system power at BER=10^{-6}.

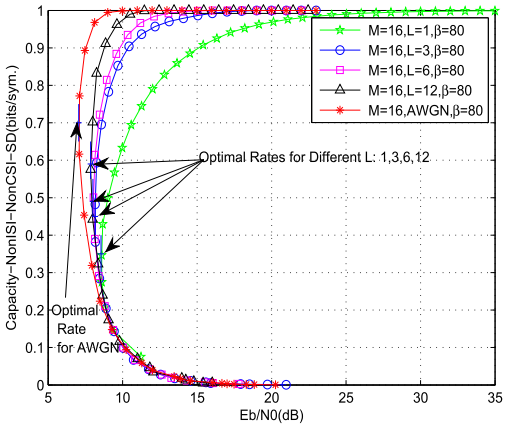

FIGURE 7. Non-capacity bounds of the M-ary DCSK system corresponding to the increasing of the path number L.

the performance at $R_c = \frac{1}{2}$ outperforms the other code rates. Hence, a U-shaped capacity bound exists. As shown in Fig. 6(b), there is a large range of optimal code rates below 1dB, 0.18∼0.80bits/sym. Meanwhile, compared with the IR and the NonIR, the derived bound is much more accurate and quantitative for the uniqueness of the capacity. When $R_c = \frac{1}{2}$, the capacity performance of the 16-ary DCSK system is about 0.2dB better than the IR system, and is about 2.2dB compared with the NonIR one. When $R_c = 0.9$, the theoretical capacity bound is much more accurate than the others, about 4.0dB gain for the IR system and about 7.2dB for the NonIR system.

Fig. 7 presents the relationship between the capacity bound and the multipath number L for the M-ary DCSK modulation system, where solid cures with "⋆", "○", "□", "△" and "∗" denote the capacity bounds based on different multipath numbers L, over AWGN channels, respectively. It is found that the optimal rate is larger when the multipath number L is increasing under the same conditions: dimension $M = 16$, spreading factor $\beta = 80$. Meanwhile, the optimal code rate (corresponds to the lowest SNR of multipath fading channels) is increasing with the heightening of L. When L is large enough ($L \to \infty$), the capacity bound coincides with the case of the AWGN channels, and the optimal code rate is the largest, where it begins with the case of $L = 1$.

C. COMPLEXITY OF M-ARY DCSK SYSTEM

A high-dimensional DCSK modulation for coherent systems achieves only a little better than that for non-coherent ones, but it is at the cost of having greatly higher complexity. Non-coherent reception system is much simpler, which offers a good tradeoff between complexity and performance, and the capacity bounds are worsened with the increase of the spreading factors. In the case of requiring low power and low complexity, the non-coherent high-dimensional DCSK systems with small spreading factors can be considered, so as to avoid the complicated chaos synchronization requirement.

V. CONCLUSIONS

The non-coherent capacity bounds of the M-ary DCSK modulation system have been derived mathematically over multipath Rayleigh fading channels in the following scenarios: CSI-SD, CSI-HD, NonCSI-SD and NonCSI-HD. Firstly, it reveals that the capacity bounds of the non-coherent reception are left-shifted (the capacity performance is improved) with the increasing of the dimension M. And the dimension's influence on the soft-decision capacity is much stronger than that is on the hard-decision one. Compared with NonISI channels, the influence of the dimension M on SD/HD capacity bounds over ISI channels is more significant. In addition, the U-shaped bounds are right-shifted (the capacity performance is worsened) as the spreading factor β increases. Besides, the influence of β on the hard-decision capacity is more significant than that is on the soft-decision over NonISI channels. It is found that there is a relatively broad range of optimal code rates in U-shaped capacity bounds. Finally, it has been shown that U-shaped capacity bounds exist by investigating the mechanism of the LDPC coded M-ary DCSK system at different code rates. When the multipath number L is larger, the optimal code rate of the M-ary DCSK system is

increasing. When L is large enough ($L \to \infty$), the capacity bound coincides with the case of the AWGN channels, meanwhile the optimal code rate is the largest, where it begins with the case of the single-path Rayleigh fading channel.

In the future, it is important to investigate the coded performance and coding optimization of M-ary DCSK/FM-DCSK systems based on some known capacity bounds over multipath fading channels.

REFERENCES

[1] G. Kolumban, "UWB technology: Chaotic communications versus noncoherent impulse radio," in *Proc. IEEE Eur. Conf. Circuit Theory Design (ECCTD)*, Sep. 2005, pp. 79–82.

[2] X. Min, W. Xu, L. Wang, and G. R. Chen, "Promising performance of a frequency-modulated differential chaos shift keying ultra-wideband system under indoor environments," *IET Commun.*, vol. 4, no. 2, pp. 125–134, Jan. 2010.

[3] G. Cimatti, R. Rovatti, and G. Setti, "Chaos-based spreading in DS-UWB sensor networks increases available bit rate," *IEEE Trans. Circuits Syst. I, Reg. Papers*, vol. 54, no. 6, pp. 1327–1339, Jun. 2007.

[4] C.-C. Chong and S. K. Yong, "UWB direct chaotic communication technology for low-rate WPAN applications," *IEEE Trans. Veh. Technol.*, vol. 57, no. 3, pp. 1527–1536, May 2008.

[5] F. C. M. Lau and C. K. Tse, *Chaos-Based Digital Communication Systems: Operating Principles, Analysis Methods, Performance Evaluation*. Berlin, Germany: Springer-Verlag, 2003.

[6] Y. Fang, L. Xu, L. Wang, and G. Chen, "Performance of MIMO relay DCSK-CD systems over Nakagami fading channels," *IEEE Trans. Circuits Syst. I, Reg. Papers*, vol. 60, no. 3, pp. 757–767, Mar. 2013.

[7] S. Ray, M. Medard, and L. Zheng, "Wideband non-coherent MIMO capacity," in *Proc. IEEE Int. Symp. Inf. Theory (ISIT)*, Adelaide, Australia, Sep. 2005, pp. 646–650.

[8] G. Kolumban, B. Vizvari, W. Schwarz, and A. Abel, "Differential chaos shift keying: A robust coding for chaotic communication," in *Proc. Int. Workshop Nonlinear Dyn. Electron. Syst. (NDES)*, Seville, Spain, Jun. 1996, pp. 87–92.

[9] W. Xu, L. Wang, and G. Kolumbán, "A new data rate adaption communications scheme for code-shifted differential chaos shift keying modulation," *Int. J. Bifurcations Chaos*, vol. 22, no. 8, pp. 1–9, Sep. 2012.

[10] G. Kaddoum, F. Gagnon, and F. D. Richardson, "Design and analysis of a multi-carrier differential chaos shift keying communication system," *IEEE Trans. Commun.*, vol. 61, no. 8, pp. 3281–3291, Aug. 2013.

[11] H. Yang, G.-P. Jiang, and J. Duan, "Phase-separated DCSK: A simple delay-component-free solution for chaotic communications," *IEEE Trans. Circuits Syst. II, Exp. Briefs*, vol. 61, no. 12, pp. 967–971, Dec. 2014.

[12] P. Chen, L. Wang, and G. Chen, "DDCSK-Walsh coding: A reliable chaotic modulation-based transmission technique," *IEEE Trans. Circuits Syst. II, Exp. Briefs*, vol. 59, no. 2, pp. 128–132, Feb. 2012.

[13] H. Yang and G. Jiang, "Reference-modulated DCSK: A novel chaotic communication scheme," *IEEE Trans. Circuits Syst. II, Express Briefs*, vol. 60, no. 4, pp. 232–236, Apr. 2013.

[14] H. Yang, W. K. Tang, G. R. Chen, and G. P. Jiang, "System design and performance analysis of orthogonal multi-level differential chaos shift keying modulation scheme," *IEEE Trans. Circuits Syst. I, Reg. Papers*, vol. 63, no. 1, pp. 146–156, Jan. 2016.

[15] L. Wang, G. Cai, and G. R. Chen, "Design and performance analysis of a new multiresolution M-ary differential chaos shift keying communication system," *IEEE Trans. Wireless Commun.*, vol. 14, no. 9, pp. 5197–5208, Sep. 2015.

[16] Z. Galias and G. M. Maggio, "Quadrature chaos-shift keying: Theory and performance analysis," *IEEE Trans. Circuits Syst. I, Fundam. Theory Appl.*, vol. 48, no. 12, pp. 1510–1519, Dec. 2001.

[17] G. Kolumbn, M. P. Kennedy, and G. Kis, "Multilevel differential chaos shift keying," in *Proc. NDES*, Moscow, Russia, Jun. 1997, pp. 191–196.

[18] G. Kis, "Performance analysis of chaotic communication systems," Ph.D. dissertation, Dept. Meas. Inf. Syst., Budapest Univ. Technol. Economics, Budapest, Hungary, 2005.

[19] A.-B. Salberg and A. Hanssen, "A subspace theory for differential chaos-shift keying," *IEEE Trans. Circuits Syst. II, Exp. Briefs*, vol. 53, no. 1, pp. 51–55, Jan. 2006.

[20] J. G. Proakis and M. Salehi, *Digital Communication*, 5th ed. New York, NY, USA: McGraw-Hill, 2008.

[21] C. Zhang, L. Wang, and G. R. Chen, "Promising performance of PA-coded SIMO FM-DCSK communication systems," *Circuits, Syst. Signal Process.*, vol. 27, no. 6, pp. 915–926, Dec. 2008.

[22] L. Wang and G. R. Chen, "Using LDPC codes to enhance the performance of FM-DCSK," in *Proc. IEEE Midwest Symp. Circuits Syst. (MSCAS)*, Hiroshima, Japan, Jul. 2004, pp. 401–404.

[23] Y. Lyu, L. Wang, G. Cai, and G. Chen, "Iterative receiver for M-ary DCSK systems," *IEEE Trans. Commun.*, vol. 63, no. 11, pp. 3929–3936, Nov. 2015.

[24] G. Cai, L. Wang, and G. R. Chen, "Capacity of the non-coherent DCSK system over Rayleigh fading channel," *Accept by IET commun.*, Aug. 2016.

[25] I. E. Telatar and D. N. C. Tse, "Capacity and mutual information of wideband multipath fading channels," *IEEE Trans. Inf. Theory*, vol. 46, no. 4, pp. 1384–1400, Jul. 2000.

[26] S. Dolinar, D. Divsalar, and J. Hamkins, "Capacity of PPM on Gaussian and Webb channels," in *Proc. IEEE Int. Symp. Inf. Theory (ISIT)*, Sorrento, Italy, Jun. 2000, p. 410.

[27] G. Cai, L. Wang, and T. Huang, "Channel capacity of M-ary differential chaos shift keying modulation over AWGN channel," in *Proc. IEEE Int. Symp. Commun. Inf. Technol. (ISCIT)*, Samui Island, Thailand, Sep. 2013, pp. 91–95.

[28] W. Hirt and J. L. Massey, "Capacity of the discrete-time Gaussian channel with intersymbol interference," *IEEE Trans. Inf. Theory*, vol. 34, no. 3, p. 38, May 1988.

[29] W. Xiang and S. S. Pietrobon, "On the capacity and normalization of ISI channels," *IEEE Trans. Inf. Theory*, vol. 49, no. 9, pp. 2263–2268, Sep. 2003.

[30] R. K. Ganti, A. Thangaraj, and A. Mondal, "Approximation of capacity for ISI channels with one-bit output quantization," in *Proc. IEEE Int. Symp. Inf. Theory (ISIT)*, Hong Kong, Jun. 2015, pp. 2316–2320.

[31] G. Taricco and J. J. Boutros, "An asymptotic approximation of the ISI channel capacity," in *Proc. IEEE Inf. Theory Appl. Workshop (ITA)*, San Diego, CA, USA, Feb. 2014, pp. 1–5.

[32] D. Arnold and H. A. Loeliger, "On the information rate of binary-input channels with memory," in *Proc. IEEE Int. Conf. Commun. (ICC)*, Helsinki, Finland, Jun. 2001, pp. 2692–2695.

[33] H. D. Pfister, J. B. Soriaga, and P. H. Siegel, "On the achievable information rates of finite state ISI channels," in *Proc. IEEE Global Commun. Conf. (GLOBECOM)*, San Antonio, TX, USA, Nov. 2001, pp. 2992–2996.

[34] A. Goldsmith, *Wireless Communications*. Cambridge, U.K.: Cambridge Univ. Press, 2005.

WEI HU received the M.Sc. degree in communication and information system from Shanghai Normal University, Shanghai, China, in 2013. He is currently pursuing the Ph.D. degree with the Department of Communication Engineering, Xiamen University, Fujian, China. His research interests include information theory and chaotic communications.

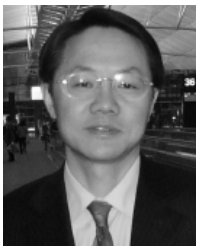

LIN WANG (S'99–M'03–SM'09) received the M.Sc. degree in applied mathematics from the Kunming University of Technology, China, in 1988, and the Ph.D. degree in electronics engineering from the University of Electronic Science and Technology of China, China, in 2001. From 1984 to 1986, he was a Teaching Assistant with the Mathematics Department, Chongqing Normal University. From 1989 to 2002, he was a Teaching Assistant, a Lecturer, and then an Associate Professor in applied mathematics and communication engineering with the Chongqing University of Post and Telecommunication, China. From 1995 to 1996, he was with the Mathematics Department, University of New England, Armidale, NSW, Australia, for one year. In 2003, he was a Visiting Researcher with the Center for Chaos and Complexity Networks, Department of Electronic Engineering, City University of Hong Kong, for three months. In 2013, he was a Senior Visiting Researcher with the Department of ECE, University of California at Davis, Davis, CA, USA. From 2003 to 2012, he was a Full Professor and an Associate Dean with the School of Information Science and Technology, Xiamen University, China. He has been a Distinguished Professor since 2012. He holds 14 patents in the field of physical layer in digital communications. He has authored over 100 journal and conference papers. His current research interests are in the area of channel coding, joint source and channel coding, chaos modulation, and their applications to wireless communication and storage systems.

GUOFA CAI received the B.Sc. degree in communication engineering from Jimei University, Xiamen, China, in 2007, the M.Sc. degree in circuits and systems from Fuzhou University, Fuzhou, China, in 2012, and the Ph.D. degree from the Department of Communication Engineering, Xiamen University, Xiamen, in 2016. He is currently with the School of Information Engineering, Guangdong University of Technology, Guangzhou, China. His primary research interests include information theory, chaotic communications, channel coding, UWB, and MIMO communications.

GUANRONG (RON) CHEN (M'89–SM'92–F'97) was a Tenured Full Professor with the University of Houston, Houston, TX, USA. He has been a Chair Professor and the Director of the Center for Chaos and Complex Networks with the City University of Hong Kong since 2000. He received the 2011 Euler Gold Medal, Russia, and conferred Honorary Doctorate by the Saint Petersburg State University, Russia, in 2011 and by the University of Le Havre, France, in 2014. He is a member of the Academy of Europe and a fellow of The World Academy of Sciences.